

# The ultrastructure of fibrinogen-420 and the fibrin-420 clot

M.W. Mosesson<sup>a,\*</sup>, J.P. DiOriob, I. Hernandez<sup>a</sup>, J.F. Hainfeld<sup>c</sup>, J.S. Wall<sup>c</sup>, G. Grieneringer<sup>d</sup>

<sup>a</sup>The Blood Research Institute of The Blood Center of Southeastern Wisconsin, PO Box 2178, Milwaukee, WI 53201-2178, USA

<sup>b</sup>Baxter Healthcare, Roundlake, IL, United States

<sup>c</sup>Biology Department, Brookhaven National Laboratory, Upton, NY, United States

<sup>d</sup>3 Washington Square Village, New York, NY 10012, United States

Received 13 April 2004; received in revised form 26 April 2004; accepted 1 July 2004

Available online 28 August 2004

## Abstract

Fibrinogen-420 is a minor subclass of human fibrinogen that is so named because of its higher molecular weight compared to fibrinogen-340, the predominant form of circulating fibrinogen. Each of the two A $\alpha$  chains of fibrinogen-340 is replaced in fibrinogen-420 by an A $\alpha$  isoform termed  $\alpha_E$ . Such chains contain a globular C-terminal extension,  $\alpha_E$ C, that is homologous with the C-terminal regions of B $\beta$  and  $\gamma$  chains in the fibrin D domain. The  $\alpha_E$ C domain lacks a functional fibrin polymerization pocket like those found in the D domain, but it does contain a binding site for  $\beta_2$  integrins. Electron microscopy of fibrinogen-340 molecules showed the major core fibrinogen domains, D–E–D, plus globular portions of the C-terminal  $\alpha$ C domains. Fibrinogen-420 molecules had two additional globular domains that were attributable to  $\alpha_E$ C. Turbidity measurements of thrombin-cleaved fibrinogen-420 revealed a reduced rate of fibrin polymerization and a lower maximum turbidity. Thromboelastographic measurements also showed a reduced rate of fibrin-420 polymerization (amplitude development) compared with fibrin-340. Nevertheless, the final amplitude (MA) and the calculated elastic modulus ( $G$ ) for fibrin-420 were greater than those for fibrin-340. These results suggested a greater degree of fibrin-420 branching and thinner matrix fibers, and such structures were found in SEM images. In addition, fibrin-420 fibers were irregular and often showed nodular structures protruding from the fiber surface. These nodularities represented  $\alpha_E$ C domains, and possibly  $\alpha$ C domains as well. TEM images of negatively shadowed fibrin-420 networks showed irregular fiber borders, but the fibers possessed the same 22.5-nm periodicity that characterizes all fibrin fibers. From this result, we conclude that fibrin-420 fiber assembly occurs through the same D–E interactions that drive the assembly of all fibrin fibrils, and therefore that the staggered overlapping molecular packing arrangement is the same in both types of fibrin. The  $\alpha_E$ C domains are arrayed on fiber surfaces, and in this location, they would very likely slow lateral fibril association, causing thinner, more branched fibers to form. However, their location on the fiber surface would facilitate cellular interactions through the integrin receptor binding site.

© 2004 Elsevier B.V. All rights reserved.

**Keywords:** Fibrin; Fibrinogen; Thrombin

## 1. Introduction

A subclass of human fibrinogen molecules termed fibrinogen-420 (reviewed in Ref. [1]) contains homodimeric A $\alpha$  isoforms termed  $\alpha_E$ , which comprise a unique 236-residue C-terminal extension termed  $\alpha_E$ C [2,3] (Fig. 1). The

human  $\alpha_E$ -containing isoform ( $\alpha_E$ , B $\beta$ ,  $\gamma$ )<sub>2</sub> amounts to 1–3% of the predominant form of fibrinogen (A $\alpha$ , B $\beta$ ,  $\gamma$ )<sub>2</sub> [4]. This isoform occurs throughout the vertebrate kingdom and is highly conserved [5,6,7]. It shares about 40% homology with comparable C-terminal  $\gamma$ C and  $\beta$ C domains [2], and its folding is largely super-imposable upon the  $\gamma$ C and  $\beta$ C constituents in the fibrinogen D domains [8]. This domain lacks the negatively charged polymerization pockets that are present in  $\gamma$ C and  $\beta$ C domains [8,9], and, therefore, it does not participate directly in the initial thrombin-mediated fibrin assembly process. It does, however, contain a recognition site for leucocyte  $\beta_2$  integrins [10] that is

*Abbreviations:* TEM, transmission electron microscopy; STEM, scanning–transmission electron microscopy; SEM, scanning electron microscopy.

\* Corresponding author. Tel.: +1 414 9373811; fax: +1 414 9376824.

E-mail address: mwmosesson@bcsew.edu (M.W. Mosesson).

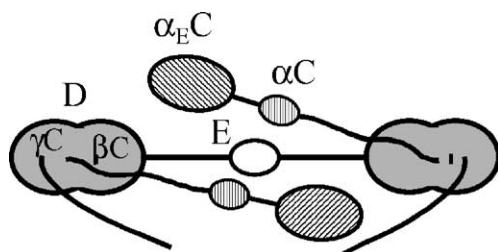


Fig. 1. Schematic drawing of a fibrinogen-420 molecule showing the location of the major domains, including the D, E,  $\alpha$ C (vertical hatched), and  $\alpha_E$ C domains (transversely hatched). Only the  $\alpha_E$ C domains are unique to fibrinogen-420 molecules.

functionally similar to the  $\alpha_M\beta_2$  (Mac-1) receptor site in the  $\gamma$ -subdomain of the fibrinogen D domain [11].

The studies to be described were initiated in an effort to characterize the ultrastructure of fibrinogen-420 molecules and the fibrin polymers derived from them. By including this report in the John D. Ferry Festschrift, we intend to recognize some of his prior achievements in this field, especially his contributions to our understanding of the staggered overlapping molecular assembly of fibrin [12].

## 2. Materials and methods

Because of the relative abundance of fibrinogen-420 in fetal blood [4], human umbilical cord plasma was chosen for preparing fibrinogen-420 and as a by-product, the more common fibrinogen-340. These variant fibrinogens were separated from each other by Mono Q anion exchange chromatography as described [13], and the final preparations had clottabilities of >95%. Turbidity measurements on thrombin-treated fibrinogen solutions were carried out in a recording spectrophotometer at 340 nm in 140 mM NaCl, 20 mM Tris, pH 7.4 buffer at a fibrinogen concentration of

0.5 mg/ml, and a thrombin concentration of 0.2 U/ml. Thromboelastographic measurements were made in a Hellige Thromboelastograph Coagulation Analyzer model 3000R (Haemoscope, Skokie, IL) at a fibrinogen concentration of 2.7 mg/in 140 mM NaCl, 20 mM Tris, pH 7.4 buffer, and a thrombin concentration of 5 U/ml. Tracings were evaluated using standard measurement parameters [14] where  $r$ =reaction time in minutes, Angle=initial slope of amplitude development in degrees, MA=maximum amplitude in millimeters, and  $G$ =modulus of elasticity derived from the MA in dynes per second.

For scanning electron microscopy (SEM), fibrin was formed directly on carbon-formvar-coated grids by adding 0.5  $\mu$ l thrombin to a 5- $\mu$ l drop of fibrinogen at 200  $\mu$ g/ml in 125 mM NaCl, 25 mM HEPES, 1 mM  $\text{CaCl}_2$ , pH 7.4 buffer (final thrombin concentration, 1 U/ml) or in 300 mM NaCl, 20 mM HEPES, 1 mM  $\text{CaCl}_2$ , pH 8.0 buffer (final thrombin concentration, 0.1 U/ml), and incubated in a humidity chamber for 3 h. The clots were fixed with 2.5% glutaraldehyde, 0.2% tannic acid, 100 mM HEPES, pH 7.0 buffer, dehydrated, critical point dried, sputter-coated with gold, and examined in a JOEL JSM6300F field emission scanning electron microscope.

For scanning-transmission electron microscopy (STEM) at the Brookhaven STEM Biotechnology Resource Facility, samples were diluted in 10 mM HEPES, 150 mM NaCl, pH 7.4 buffer to a concentration of 5  $\mu$ g/ml. Three microliters of sample was injected into a 3- $\mu$ l droplet of sample buffer on a grid covered with an ultrathin carbon film, allowed to attach to the grid surface for 1 min, and followed by multiple wicking/washing exchanges with 150 mM ammonium acetate, pH 7. The grid was then snap frozen in degassed liquid nitrogen, freeze-dried, transferred to the STEM microscope stage under vacuum, and imaged using a 40-kV probe focused at 0.25 nm. Background filtering of digitized STEM images was optimized for brightness and

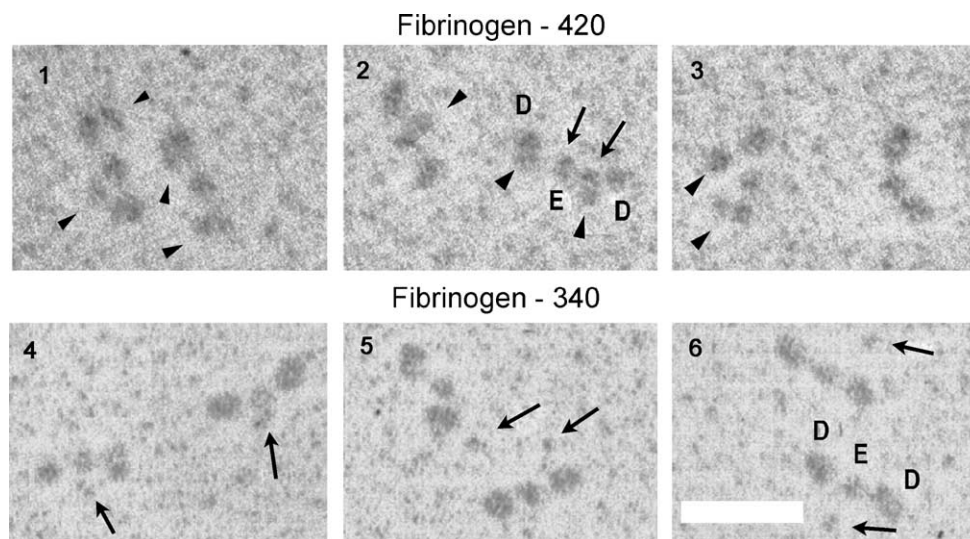


Fig. 2. A gallery of images of metal-shadowed fibrinogen-420 (panels 1–3) and fibrinogen-340 molecules (panels 4–6). The D and E domains of selected molecules are indicated. Arrowheads point to  $\alpha_E$ C domains; arrows, to  $\alpha$ C domains. Bar, 50 nm.

contrast offset by an image processing program (Adobe Photoshop). Mass measurements of STEM images were based on electron scattering measurements and were performed off-line [15].

Fibrinogen samples for rotary shadowing were diluted to 30  $\mu\text{g/ml}$  in 30% glycerol, 0.15 M ammonium acetate, pH 7, sprayed onto mica discs, rotary-shadowed with carbon-platinum and examined in a Philips 400 transmission electron microscope (TEM) at 60 kV. Negatively contrasted images of fibrin networks were obtained from specimens that had been deposited on carbon-formvar-coated grids at a fibrinogen concentration of 50  $\mu\text{g/ml}$  in 100 mM NaCl, 50 mM Tris, pH 7.4 buffer, then converted to fibrin by adding thrombin at a final concentration of 1 U/ml, negatively contrasted with 2% uranyl acetate, and then examined in a JOEL 1200-EX at 80 kV.

### 3. Results and discussion

#### 3.1. Electron microscopic images of fibrinogen

Metal-shadowed fibrinogen-340 molecules showed three core globular domains representing the two outer D domains and the central E domain, of which all fibrinogen molecules are comprised (Fig. 2, panels 4–6). A less prominent globular structure, commonly located near the E domain (arrows), represented the globular portion of the  $\alpha\text{C}$  domains (arrows) [16]. In contrast, shadowed images of fibrinogen-420 molecules (panels 1–3) showed the usual D and E domains, plus two additional structures that were attributable to the  $\alpha_{\text{E}}\text{C}$  domains (arrowheads) in each molecule, and two others representing the  $\alpha\text{C}$  domains. It was usually easy to distinguish structures representing  $\alpha_{\text{E}}\text{C}$  domains from the D and E domains of the molecule since most commonly they were not aligned with the core D–E–D fibrinogen domains, and their longest dimension was somewhat smaller than that of the D domains ( $\sim 6\text{--}7$  nm versus  $\sim 9$  nm). When

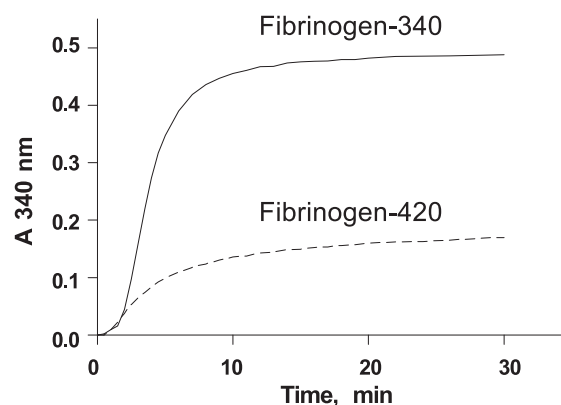


Fig. 4. Turbidity measurements on thrombin-treated fibrinogen-340 and fibrinogen-420 made at 340 nm in 140 mM NaCl, 20 mM Tris, pH 7.4 buffer.

identifiable, the globular portion of the  $\alpha\text{C}$  domain (arrows) could be visualized near to a  $\alpha_{\text{E}}\text{C}$  domain (panel 2), and  $\alpha_{\text{E}}\text{C}$  domains were generally located near to a D domain, sometimes overlapping them to such an extent that they were not distinguishable from them (panel 3, right image).

Mass measurements on STEM images of fibrinogen-420 molecules (Fig. 3) validated our interpretation of the composition of these structures in that isolated fibrinogen-420 molecules yielded a mass of  $426 \pm 67$  kDa ( $n=22$ ) versus  $322 \pm 28$  kDa ( $n=17$ ) for fibrinogen-340 molecules. The general arrangement of the several domains in fibrinogen-420 was the same as had been observed in the shadowed images, except that the ovoid  $\alpha_{\text{E}}\text{C}$  domains (long dimension  $\sim 7\text{--}8$  nm) were often situated further from the parent fibrinogen molecules than had been observed in shadowed images. Sometimes  $\alpha_{\text{E}}\text{C}$  domains overlapped one another (panel 3). We were not able to visualize the peptide ‘stalks’ that connected the D domains (long dimension  $\sim 9\text{--}10$  nm) with its  $\alpha_{\text{E}}\text{C}$  domains, presumably because their electron density was not detectable above that of the background carbon film. This is similar to the situation with the coiled-coil segments connecting D and E

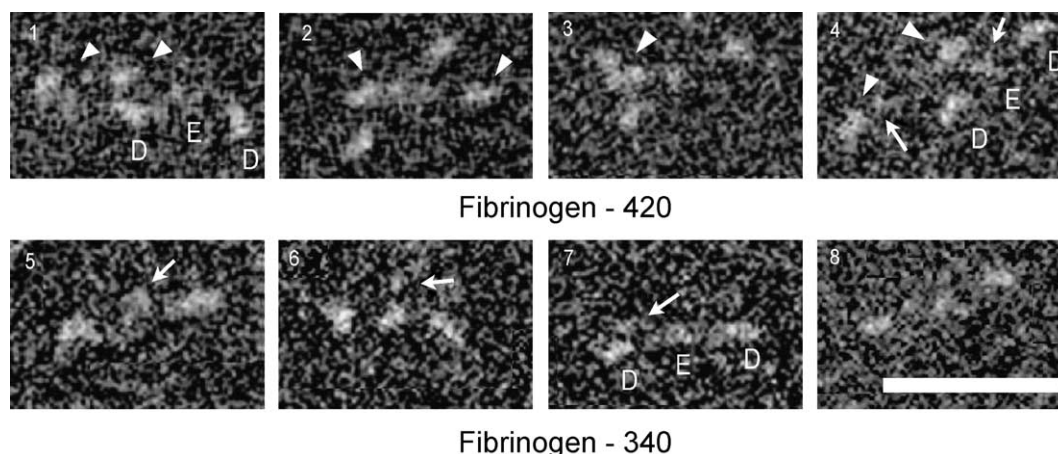


Fig. 3. A gallery of STEM images of fibrinogen-420 molecules (panels 1–4) and fibrinogen-340 molecules (panels 5–8). The D and E domains of selected molecules are indicated. Arrowheads point to  $\alpha_{\text{E}}\text{C}$  domains; arrows, to  $\alpha\text{C}$  domains. Bar, 50 nm.



Table 1  
Thromboelastography

Fibrinogen preparation	<i>n</i>	<i>r</i> , min	Angle, °	MA, mm	<i>G</i> , dynes/s
Fibrinogen-420	2	0.5	51	26	1758
Fibrinogen-340	2	0.5	80	23	1496

*n*, Number of determinations; *r*, reaction time, min; Angle, the slope of amplitude development; MA, maximum amplitude; *G*, modulus of elasticity.

domains [17,18]. Smaller globular structures, ~4–6 nm, representing globular portions of  $\alpha$ C domains (arrows) could often be identified in fibrinogen-420 molecules and were situated near to a  $\alpha$ <sub>E</sub>C domain. In fibrinogen-340 molecules,  $\alpha$ C domains were readily identified.

### 3.2. Turbidity measurements and thromboelastography

Turbidity measurements on thrombin-treated fibrinogen-420 revealed that both the polymerization rate and

the final extent of turbidity development were lower than those of the control, fibrin-340 (Fig. 4). The observations are similar to those reported by Applegate et al. [13], although at the time of their report, the curves were believed not to differ significantly. Thromboelastographic measurements (Table 1) supported and extended these observations. The '*r*' for fibrinogen-420, corresponding to the gelation or clotting time, was the same for both fibrinogen variants, implying that initial fibrin assembly was the same for both types. However, the rate of polymerization of fibrin-420 was lower than that of fibrin-340 (angle, 51° versus 80°), indicating slower matrix assembly for fibrin-420. In any case, the final amplitude (MA) of fibrin-420 was higher than that for fibrin-340 and was reflected in the higher value calculated for the elastic modulus (*G*). We believe that the basis for this difference is related to the higher degree of branching of the fibrin-420 matrix, and this premise was verified from SEM images (see below).

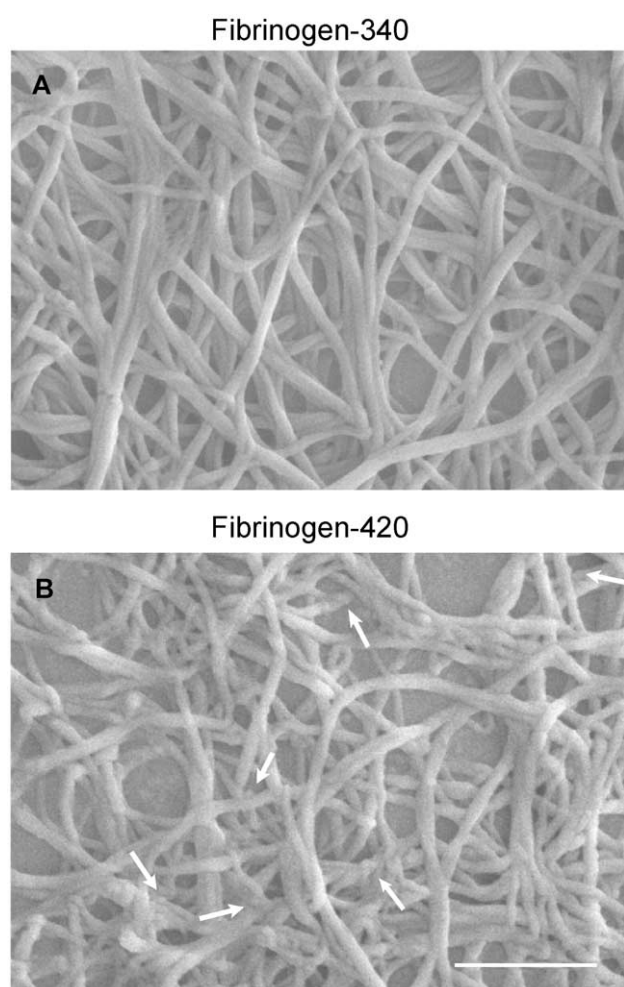


Fig. 5. SEM images of fibrin-340 (panel A) and fibrin-420 (panel B) prepared in 125 mM NaCl, 25 mM HEPES, 1 mM CaCl<sub>2</sub>, pH 7.4 buffer at a final thrombin concentration of 1 U/ml. The arrows indicate nodular structures. Bar, 1  $\mu$ M.

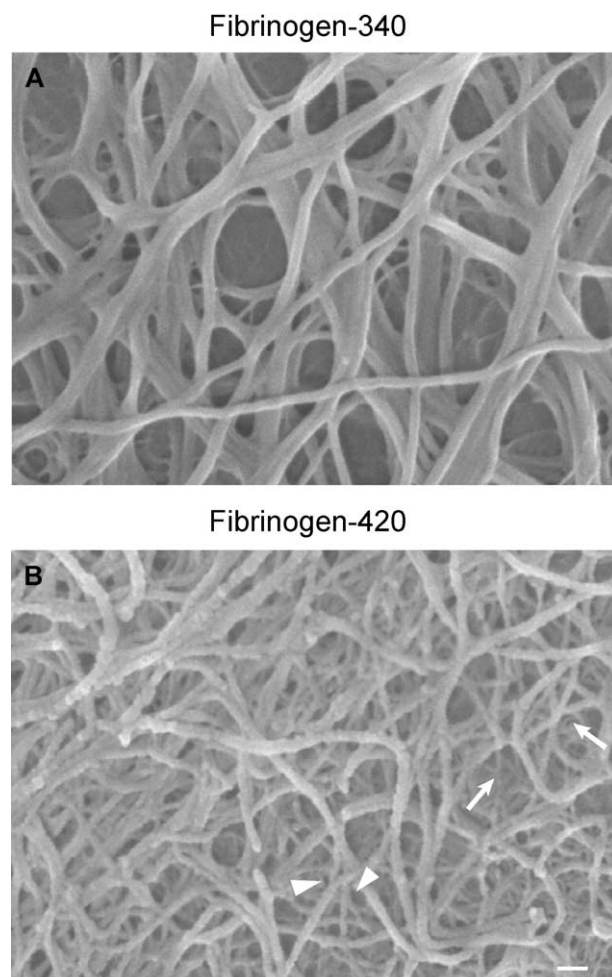


Fig. 6. SEM images of fibrin-340 (panel A) and fibrin-420 (panel B) prepared in 300 mM NaCl, 20 mM HEPES, 1 mM CaCl<sub>2</sub>, pH 8.0 buffer at a final thrombin concentration of 0.1 U/ml. The arrows indicate 'equilateral' branch junctions; arrowheads indicate 'tetramolecular' branch junctions. Bar, 100 nm.

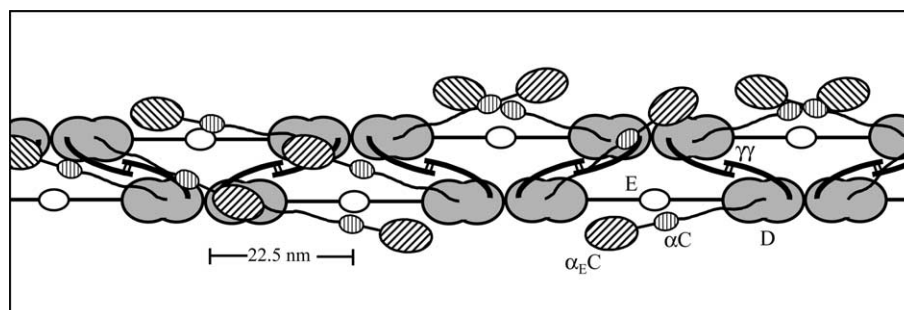


Fig. 7. Schematic drawing of a fibrin-420 fibril. The staggered overlapping molecular arrangement in this fibril is characteristic of all fibrin fibrils, as proposed many years ago by John Ferry [12]. The C-terminal regions of the  $\gamma$  chains ( $\gamma\gamma$ ) in this fibril are situated transversely between each fibril strands, as recently discussed [20], and are depicted as having been cross-linked by factor XIIIa. The  $\alpha_E C$  and  $\alpha C$  domains are arrayed on the outside of the fibril.

### 3.3. SEM images of fibrin-420 and fibrin-340

The SEM structure of the fibrin-420 matrix differed significantly from that of fibrin-340 in that fibrin-420 fibers were thinner and more branched than those of fibrin-340 (Fig. 5). In addition, fibrin-420 fibers formed at pH 7.4 and 125 mM NaCl were considerably more irregular than fibrin-340 fibers, and often contained nodular structures protruding from their surface (arrows) that accounted for the fiber irregularities. These nodular structures, most likely representing  $\alpha_E C$  or  $\alpha C$  domains, or both, were considerably more obvious in matrices formed at 300 mM NaCl and pH 8.0 (Fig. 6). A diagram showing the arrangement of these structures in a fibrin fibril is presented in Fig. 7.

Under the high salt conditions depicted in Fig. 6, fibrin fibers were thinner than those formed at pH 7.4 and fibrin-420 fibers were extensively studded with surface globular structures. The widths of the thinnest fibrin-420 fibrils (no corrections for the metal coating) was  $\sim 25$  to 50 nm, suggesting that such fibrils were comprised of either two or four strands. ‘Equilateral’ branch junctions (arrows) [19] (a junction with three contributing fibrils of equal width) found in the thinnest fibrils further suggested that such structures were double-stranded. There were also numerous examples

of ‘tetramolecular’ branch junctions [typically, a four-stranded fibril diverging to two double-stranded fibrils (arrowheads)].

### 3.4. Negatively contrasted images of fibrin-420 and fibrin-340 fibers

To investigate whether  $\alpha_E C$  domains were exclusively surface-oriented structures, we examined negatively shadowed images of fibrin-340 and fibrin-420 (Fig. 8). Images of fibrin-340 fibers were regular with well-defined outer margins and sharply delineated periodic striations having the 22.5 nm spacing that is typical of assembled fibrin. Only occasional small globular structures ( $\sim 9$  nm) could be identified on the fibrin-340 fibers (arrows), and they probably reflected the globular portions of  $\alpha C$  domains. The outer margins of negatively contrasted fibrin-420 fibers (panel B) were less regular than fibrin-340 fibers and globular structures (arrows) similar to those seen in SEM fiber images were readily identified. These globular structures were most readily appreciated when they were overlying fibers that did not show good stain penetration (inset, panel B). The widths of these globular structures was  $\sim 20$  nm, suggesting that they might be comprised of more

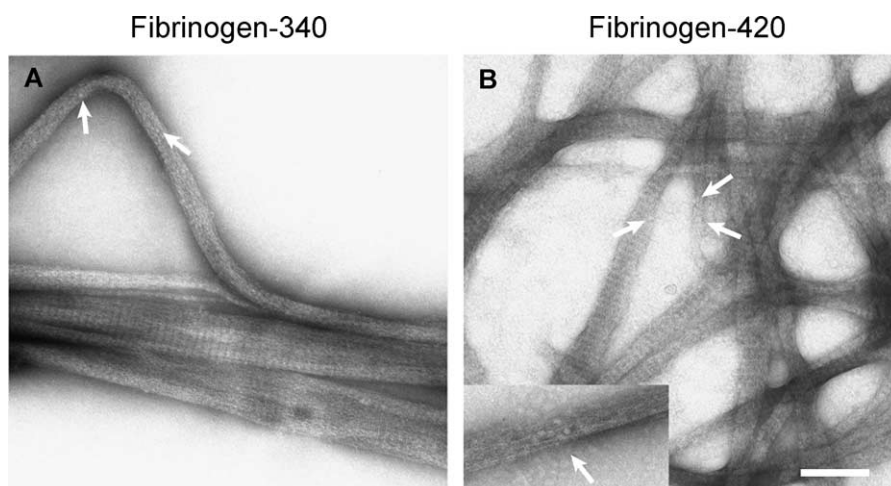


Fig. 8. Negatively contrasted images of fibrin-340 (panel A) or fibrin-420 (panel B and inset) fibers. The globular structures (arrows) were most readily appreciated when they overlaid fibers that did not show good stain penetration (inset, panel B). Bar, 200 nm.

than a single  $\alpha_E C/\alpha C$  domain (cf. STEM images of fibrinogen-420  $\alpha_E C$  and  $\alpha C$  domains, Fig. 3). Owing to the overlying structures on the fiber surface, the periodic banding of fibrin-420 fibers seemed to be somewhat less prominent than the sharp banding pattern observed in fibrin-340 fibers (cf. panels A and B). More importantly, the 22.5 nm repeat in fibrin-420 was the same as that in fibrin-340, indicating that the molecular packing arrangement in the fibrin-420 fiber was the same as that in fibrin-340. This confirmed earlier SEM observations indicating that  $\alpha_E C$  domains were located on the fiber surface.

Our findings indicate that following proteolytic cleavage by thrombin, fibrin-420 molecules assemble through the same intermolecular interactions between D and E domains (D–E) that cause the staggered overlapping end-to-middle molecular packing arrangement that is characteristic of all fibrin fibers. This arrangement was predicted by John Ferry more than 50 years ago [12]. The difference between fibrin-420 and fibrin-340 fibrils is that the  $\alpha_E C$  domains in fibrin-420 occupy the fiber surface, and probably slow the lateral fibril assembly process, resulting in a more highly branched network containing thinner fibers. The  $\alpha_E C$  domains have been conserved throughout the vertebrate kingdom, from Lamprey to humans, and we therefore presume that this structure serves an important function(s). Based upon our present knowledge, the most likely function for these domains is to provide sites for interaction with cellular integrins, and their surface location positions them well for this purpose.

## Acknowledgements

This work was supported by NIH grant HL-59507 (to MWM), HL-51050 (to GG), and an American Heart Association grant to GG.

## References

- [1] G. Grieneringer, Contribution of the  $\alpha_E C$  domain to the structure and function of fibrinogen-420, *Ann. N.Y. Acad. Sci.* 936 (2001) 44–64.
- [2] Y. Fu, L. Weissbach, P.W. Plant, C. Oddoux, Y. Cao, T.J. Liang, S.N. Roy, C.M. Redman, G. Grieneringer, Carboxy-terminal-extended variant of the human fibrinogen alpha subunit: a novel exon conferring marked homology to beta and gamma subunits, *Biochemistry* 31 (1992) 11968–11972.
- [3] Y. Fu, G. Grieneringer, Fib420: a normal variant of fibrinogen with two extended  $\alpha$  chains, *Proc. Natl. Acad. Sci. U. S. A.* 91 (1994) 2625–2628.
- [4] G. Grieneringer, X. Lu, Y. Cao, Y. Fu, B.J. Kudryk, D.K. Galanakis, K.M. Hertzberg, Fib420, the novel fibrinogen subclass: newborn levels are higher than adult, *Blood* 90 (1997) 2609–2614.
- [5] L. Weissbach, G. Grieneringer, Bipartite mRNA for chicken alpha-fibrinogen potentially encodes an amino acid sequence homologous to beta- and gamma-fibrinogens, *Proc. Natl. Acad. Sci. U. S. A.* 87 (1990) 5198–5202.
- [6] Y. Fu, Y. Cao, K.M. Hertzberg, G. Grieneringer, Fibrinogen a genes: conservation of bipartite transcripts and carboxy-terminal-extended subunits in vertebrates, *Genomics* 30 (1995) 71–76.
- [7] Y. Pan, R.F. Doolittle, cDNA sequence of a second fibrinogen alpha chain in lamprey: an archetypal version alignable with full-length beta and gamma chains, *Proc. Natl. Acad. Sci. U. S. A.* 89 (1992) 2066–2070.
- [8] G. Spraggon, D. Applegate, S.J. Everse, J.Z. Zhang, L. Veerapandian, C. Redman, R.F. Doolittle, G. Grieneringer, Crystal structure of a recombinant alphaEC domain from human fibrinogen-420, *Proc. Natl. Acad. Sci. U. S. A.* 95 (1998) 9099–9104.
- [9] D. Applegate, L. Haraga, K.M. Hertzberg, L.S. Steben, J.Z. Zhang, C.M. Redman, G. Grieneringer, The  $\alpha_E C$  domains of human fibrinogen-420 contain calcium binding sites but lack polymerization pockets, *Blood* 92 (1998) 3669–3674.
- [10] V.K. Lishko, V.P. Yakubenko, K.M. Hertzberg, G. Grieneringer, T.P. Ugarova, The alternatively spliced alpha(E)C domain of human fibrinogen-420 is a novel ligand for leukocyte integrins alpha(M)-beta(2) and alpha(X)beta(2), *Blood* 98 (2001) 2448–2455.
- [11] T.P. Ugarova, D.A. Solovjov, L. Zhang, D.I. Loukinov, V.C. Yee, L.V. Medved, E.F. Plow, Identification of a novel recognition sequence for integrin  $\alpha$ Mb2 within the g-chain of fibrinogen, *J. Biol. Chem.* 273 (1998) 22519–22527.
- [12] J.D. Ferry, The mechanism of polymerization of fibrinogen, *Proc. Natl. Acad. Sci. U. S. A.* 38 (1952) 566–569.
- [13] D. Applegate, L.S. Steben, K.M. Hertzberg, G. Grieneringer, The alpha(E)C domain of human fibrinogen-420 is a stable and early plasmin cleavage product, *Blood* 95 (2000) 2297–2303.
- [14] C.I. Traverso, J.A. Caprini, J.I. Arcelus, The normal thromboelastogram and its interpretation, *Semin. Thromb Hemost.* 21 (Suppl. 4) (1995) 7–13.
- [15] J.S. Wall, J.F. Hainfeld, Mass mapping with the scanning transmission microscope, *Annu. Rev. Biophys. Biophys. Chem.* 15 (1986) 355–376.
- [16] Y.I. Veklich, O.V. Gorkun, L.V. Medved, W. Niewenhuizen, J.W. Weisel, Carboxyl-terminal portions of the  $\alpha$  chains of fibrinogen and fibrin, *J. Biol. Chem.* 268 (1993) 13577–13585.
- [17] M.W. Mosesson, J.F. Hainfeld, R.H. Haschemeyer, J.S. Wall, Identification and mass analysis of human fibrinogen molecules and their domains by scanning transmission electron microscopy, *J. Mol. Biol.* 153 (1981) 695–718.
- [18] M.W. Mosesson, K.R. Siebenlist, J.F. Hainfeld, J.S. Wall, The covalent structure of factor XIIIa crosslinked fibrinogen fibrils, *J. Struct. Biol.* 115 (1995) 88–101.
- [19] M.W. Mosesson, J.P. DiOrio, K.R. Siebenlist, J.S. Wall, J.F. Hainfeld, Evidence for a second type of fibril branch point in fibrin polymer networks, the trimolecular junction, *Blood* 82 (1993) 1517–1521.
- [20] M.W. Mosesson, The fibrin cross-linking debate—cross-linked g chains in fibrin fibrils bridge ‘transversely’ between strands: yes, *Thromb. Haemost.* 2 (2004) 388–393.